LINEAR BEHAVIORS OF SHALLOW TRANSLATIONAL SHELLS WITH PINNED SUPPORT ALONG EDGES

Youichi MINAKAWA, Toshiaki UCHIYAMA* and Takashi NORIMATSU*

(Received May 31, 1983)

The objective of this paper is to study the effects of curvature and Poisson's ratio upon the behaviors of shallow translational shells with pinned support along edges. The shells are chosen to have two independent radii of curvature. By applying the Galerkin's procedure, the static analyses under uniform hydropressure load and the natural frequency analyses are performed. The numerical results are presented.

1. Introduction

The shallow translational shells are usually examined by basing on the Marguerre-Vlasov equation. The equation is able to be analyzed by using generalized Levy-type solution[7]. The analytical method permits us to get static behaviors under various boundary conditions[1)~4)]. Adopting the method, Yokoo and Kunieda[4),5)]presented the procedure to obtain the strict natural frequencies of shallow shells and indicated[5)]that the solution of the frequency equation for the case was not easily amenable to numerical calculations.

Then, supposing one vibration mode, the explicit expression[6),8)]for natural frequency of shallow shells was reported and effects of curvatures upon natural frequencies were assessed. The explicit expression is the solution under the boundary condition with inplane inconstraint, and brings interesting results[8)]that the fundamental natural frequency for hyperbolic paraboloidal shell is the same as for a plate.

The objective of here is to search natural frequencies for flexural vibrations of shallow shells under the boundary condition with strict inplane constraint and examine effects of curvature and Poisson's ratio upon them. For a solving method, we adopt the Galerkin's method. The method is applicable to both the static and the natural frequency analyses. For the latter case, it is considered that the Galerkin's method have an advantage to the formentioned analytical method.

2. Basic Equations for Shallow Translational Shells

The mid-surface of the translational shallow shells examined here are given by

$$Z(x, y)=\frac{1}{2}\left\{\frac{x(x-a)}{R_x}+\frac{y(y-b)}{R_y}\right\} \tag{1}$$

where x, y, z are the cartesian coordinates, and R_x and R_y are constants identifying the radii of curvature in the x and y directions, respectively. The shells have a rectangular planform of dimensions $a\times b$ with boundaries along $x=0$, a and $y=0$, b illustrated in Fig. 1. The expression (1) represents various sets of shape included in spherical shells $R_x=R_y$, cylindrical shells $R_xR_y=0$, and hyperbolic paraboloidal shells $R_x=-R_y$.

* Graduate Student, Department of Architecture, Kagoshima University

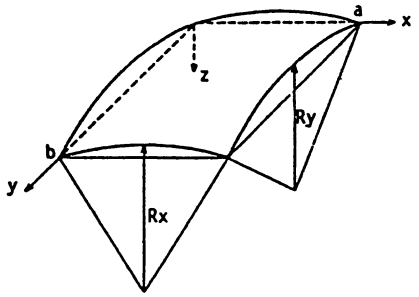

Fig. 1 Geometry of Shells

Without tangential inertia force, the linear equations of motion for shallow shells[6] in terms of the normal displacement w and the Airy's stress function Φ are generalized to

$$L(w,\ \Phi)=D\nabla^2\nabla^2 w+\frac{1}{R_x}\frac{\partial^2\Phi}{\partial y^2}+\frac{1}{R_y}\frac{\partial^2\Phi}{\partial x^2}+\rho h\frac{\partial^2 w}{\partial t^2}-p=0 \tag{2-a}$$

$$\frac{1}{Eh}\nabla^2\nabla^2\Phi-\frac{1}{R_x}\frac{\partial^2 w}{\partial y^2}-\frac{1}{R_y}\frac{\partial^2 w}{\partial x^2}=0 \tag{2-b}$$

where h=shell thickness, E=Young's modulus, ρ=mass density, ν=Poisson's ratio and $D=Eh^3/12(1-\nu^2)$. The membrane stress resultants N_x, N_y, N_{xy}, the bending and the twisting moments M_x, M_y, M_{xy}, and the inplane displacement components u and v corresponding to x and y directions, respectively are given by

$$N_x=\frac{\partial^2\Phi}{\partial y^2},\quad N_y=\frac{\partial^2\Phi}{\partial x^2},\quad N_{xy}=-\frac{\partial^2\Phi}{\partial x\partial y} \tag{3-a}$$

$$M_x=-D\left(\frac{\partial^2 w}{\partial x^2}+\nu\frac{\partial^2 w}{\partial y^2}\right),\quad M_y=-D\left(\frac{\partial^2 w}{\partial y^2}+\nu\frac{\partial^2 w}{\partial x^2}\right),\quad M_{xy}=-D(1-\nu)\frac{\partial^2 w}{\partial x\partial y} \tag{3-b}$$

$$u=\int\left\{\frac{1}{Eh}\left(\frac{\partial^2\Phi}{\partial y^2}-\nu\frac{\partial^2\Phi}{\partial x^2}\right)+\frac{w}{R_x}\right\}dx \tag{3-c}$$

$$v=\int\left\{\frac{1}{Eh}\left(\frac{\partial^2\Phi}{\partial x^2}-\nu\frac{\partial^2\Phi}{\partial y^2}\right)+\frac{w}{R_y}\right\}dy \tag{3-d}$$

In order to examine the curvature effects on linear behaviors of shallow shells with pinned support, we analyzed Eq. (2) under the following boundary conditions

$w=M_x=0$ and $u=v=0$ at $x=0$ and a (4-a, b)

$w=M_y=0$ and $u=v=0$ at $y=0$ and b (4-c, d)

Applying the Galerkin's method to Eq. (2), we derive ordinary differential equations of motion for shallow shells.

3. Procedures to Analyze the Shells with Inplane Constraint

The normal displacement w under the conditions given by Eqs. (4-a, c) is assumed by

$$w(x,\ y,\ t)=\sum_m\sum_n w_{mn}(t)\sin\alpha_m x\sin\beta_n y \tag{5}$$

where $\alpha_m=m\pi/a$, $\beta_n=n\pi/b$. In order to simplify the analysis, we restrict the case where the normal displacement is symmetric with respect to $x=a/2$ and $y=b/2$, i.e. integers m and n take odd numbers, which is the most important displacement mode for the shells. Substituting Eq. (5)

into Eq. (2—b), we have a particular solution Φ_p for the stress function

$$\Phi_p(x,y)=\frac{Eha^2}{R_x}\sum_m\sum_n\frac{(\gamma^2n^2+\lambda m^2)}{(m^2+\gamma^2n^2)^2\pi^2}w_{mn}\sin\alpha_m x\sin\beta_n y \tag{6}$$

where $\gamma=a/b$ and $\lambda=R_x/R_y$. The homogeneous solution Φ_h for the stress function is assumed by

$$\Phi_h(x,y)=\frac{Eha^2}{R_x}\Big[\sum_m\Big\{A^m{}_1\cosh\alpha_m\Big(y-\frac{b}{2}\Big)+A^m{}_3\alpha_m\Big(y-\frac{b}{2}\Big)\sinh\alpha_m\Big(y-\frac{b}{2}\Big)\Big\}\sin\alpha_m x$$
$$+\sum_n\Big\{B^n{}_1\cosh\beta_n\Big(x-\frac{a}{2}\Big)+B^n{}_3\beta_n\Big(x-\frac{a}{2}\Big)\sinh\beta_n\Big(x-\frac{a}{2}\Big)\Big\}\sin\beta_n y\Big] \tag{7}$$

Substituting the general solution for the stress function $\Phi=\Phi_p+\Phi_h$ and w into Eq. (3—c, d), and integrating the equation, we may get $u(x,y)$ and $v(x,y)$.

$$u(x,y)=\frac{a}{R_x}\Big[-\sum_m\sum_n\frac{w_{mn}}{m\pi}\Big\{\frac{\gamma^2n^2+\lambda m^2}{(m^2+\gamma^2n^2)^2}(\nu m^2-\gamma^2n^2)+1\Big\}\cos\alpha_m x\sin\beta_n y$$
$$-\sum_m m\pi\Big[\Big\{A^m{}_1(1+\nu)+2A^m{}_3\Big\}\cosh\alpha_m\Big(y-\frac{b}{2}\Big)+A^m{}_3(1+\nu)\alpha_m\Big(y-\frac{b}{2}\Big)\sinh\alpha_m\Big(y-\frac{b}{2}\Big)\Big]\cos\alpha_m x$$
$$-\sum_n\gamma n\pi\Big[\Big\{B^n{}_1(1+\nu)-B^n{}_3(1-\nu)\Big\}\sinh\beta_n\Big(x-\frac{a}{2}\Big)+B^n{}_3(1+\nu)\beta_n\Big(x-\frac{a}{2}\Big)\cosh\beta_n\Big(x-\frac{a}{2}\Big)\Big]\sin\beta_n y \tag{7—a}$$

$$v(x,y)=\frac{a}{R_x}\Big[-\sum_m\sum_n\frac{w_{mn}}{\gamma n\pi}\Big\{\frac{\gamma^2n^2+\lambda m^2}{(m^2+\gamma^2n^2)^2}(\nu\gamma^2n^2-m^2)+\lambda\Big\}\sin\alpha_m x\cos\beta_n y$$
$$-\sum_m m\pi\Big[\Big\{A^m{}_1(1+\nu)-A^m{}_3(1-\nu)\Big\}\sinh\alpha_m\Big(y-\frac{b}{2}\Big)+A^m{}_3(1+\nu)\alpha_m\Big(y-\frac{b}{2}\Big)\cosh\alpha_m\Big(y-\frac{b}{2}\Big)\Big]\sin\alpha_m x$$
$$-\sum_n\gamma n\pi\Big[\Big\{B^n{}_1(1+\nu)+2B^n{}_3\Big\}\cosh\beta_n\Big(x-\frac{a}{2}\Big)+B^n{}_3(1+\nu)\beta_n\Big(x-\frac{a}{2}\Big)\sinh\beta_n\Big(x-\frac{a}{2}\Big)\Big]\cos\beta_n y \tag{7—b}$$

At the boundaries $x=0$ and $y=0$, we have

$$u(x,0)=-\frac{a}{R_x}\sum_m m\pi\Big[\Big\{A^m{}_1(1+\nu)+2A^m{}_3\Big\}\cosh\frac{m\pi}{2\gamma}+A^m{}_3(1+\nu)\frac{m\pi}{2\gamma}\sinh\frac{m\pi}{2\gamma}\Big]\cos\alpha_m x \tag{8—a}$$

$$v(x,0)=\frac{a}{R_x}\Big[-\sum_m\sum_n\frac{w_{mn}}{\gamma n\pi}\Big\{\frac{\gamma^2n^2+\lambda m^2}{(m^2+\gamma^2n^2)^2}(\nu\gamma^2n^2-m^2)+\lambda\Big\}\sin\alpha_m x$$
$$+\sum_m m\pi\Big[\Big\{A^m{}_1(1+\nu)-A^m{}_3(1-\nu)\Big\}\sinh\frac{m\pi}{2\gamma}+A^m{}_3(1+\nu)\frac{m\pi}{2\gamma}\cosh\frac{m\pi}{2\gamma}\Big]\sin\alpha_m x$$
$$-\sum_n\gamma n\pi\Big[\Big\{B^n{}_1(1+\nu)+2B^n{}_3\Big\}\cosh\beta_n\Big(x-\frac{a}{2}\Big)+B^n{}_3(1+\nu)\beta_n\Big(x-\frac{a}{2}\Big)\sinh\beta_n\Big(x-\frac{a}{2}\Big)\Big]\Big] \tag{8—b}$$

$$v(0,y)=-\frac{a}{R_x}\sum_n\gamma n\pi\Big[\Big\{B^n{}_1(1+\nu)+2B^n{}_3\Big\}\cosh\frac{\gamma n\pi}{2}+B^n{}_3(1+\nu)\frac{\gamma n\pi}{2}\sinh\frac{\gamma n\pi}{2}\Big]\cos\beta_n y \tag{8—c}$$

$$u(0,y)=\frac{a}{R_x}\Big[-\sum_m\sum_n\frac{w_{mn}}{m\pi}\Big\{\frac{\gamma^2n^2+\lambda m^2}{(m^2+\gamma^2n^2)^2}(\nu m^2-\gamma^2n^2)+1\Big\}\sin\beta_n y$$
$$-\sum_m m\pi\Big[\Big\{A^m{}_1(1+\nu)+2A^m{}_3\Big\}\cosh\alpha_m\Big(y-\frac{b}{2}\Big)+A^m{}_3(1+\nu)\alpha_m(y-\frac{b}{2})\sinh\alpha_m\Big(y-\frac{b}{2}\Big)\Big]$$
$$+\sum_m\gamma n\pi\Big[\Big\{B^n{}_1(1+\nu)-B^n{}_3(1-\nu)\Big\}\sinh\frac{\gamma n\pi}{2}+B^n{}_3(1+\nu)\frac{\gamma n\pi}{2}\cosh\frac{\gamma n\pi}{2}\Big]\sin\beta_n y\Big] \tag{8—d}$$

The boundary conditions $u(x,0)=0$ and $v(0,y)=0$ require the following equations

$$\Big\{A^m{}_1(1+\nu)+2A^m{}_3\Big\}\cosh\frac{m\pi}{2\gamma}+A^m{}_3(1+\nu)\frac{m\pi}{2\gamma}\sinh\frac{m\pi}{2\gamma}=0 \quad \text{for each m} \tag{9—a}$$

$$\{B^n_1(1+\nu)+2B^n_3\}\cosh\frac{\gamma n\pi}{2}+B^n_3(1+\nu)\frac{\gamma n\pi}{2}\sinh\frac{\gamma n\pi}{2}=0 \quad \text{for each n} \tag{9—b}$$

When Eq. (9—a) is satisfied, $u(0\ ,\ y)$ which is symmetric with respect to $y=b/2$ vanishes at $y=0$. Then, the second term of Eq. (8—d) is able to be expanded in Fourier sine series over the closed interval $[0\ ,\ b]$, which does not involve Gibbs' phenomenon. Finally, we establish the following Fourier series

$$u(0\ ,\ y)=\frac{a}{R_x}\sum_n \tilde{u}_n\sin\beta_n y \tag{10}$$

Since the boundary condition in Eq. (4—b) requires that $u(0\ ,\ y)=0$, we find

$$\tilde{u}_n=0 \quad \text{for each n} \tag{11—a}$$

Similarly, Eq. (8—b) can be expressed by

$$v(x\ ,\ 0)=\frac{a}{R_x}\sum_m \tilde{v}_m\sin\alpha_m x$$

The requirement that $v(x\ ,\ 0)=0$ yields

$$\tilde{v}_m=0 \quad \text{for each m} \tag{11—b}$$

Setting the number of serial numbers m, n=1, 3, 5, . . . , 2N−1, we can express Eqs. (9—a, b) and (11—a, b) in matrix form

$$[S]\{c\}=[F]\{d\} \tag{12}$$

where $\{c\}=\{A_1{}^2A_3{}^1B_1{}^1B_3{}^1A_1{}^3A_3{}^3\ \cdots\ \}$, $\{d\}=\{w_{11}w_{13}w_{31}\ \cdots\ \}$. The expression guarantees the inplane constraint along edges.

Applying the Galerkin's method to Eq. (2—a), we have

$$\frac{R^2_x}{Eh}\frac{4}{ab}\int_0^a\int_0^b L(w,\Phi)\sin\alpha_{\tilde{m}}x\sin\beta_{\tilde{n}}y\,dx\,dy=0 \quad \text{for each } \tilde{m},\tilde{n} \tag{13}$$

where $\tilde{m}, \tilde{n}=1, 3, 5, \ldots, 2N-1$. Representing Eq. (13) in matrix form, we have

$$\frac{\rho R^2_x}{E}[I]\{\ddot{d}\}+[G_1G_2]\begin{Bmatrix} d \\ c \end{Bmatrix}=\{P\} \tag{14}$$

where $\ddot{}$ denotes differential with respect t.

Substituting Eq. (12) into Eq. (14), we get the following ordinary differential equation of motion.

$$\frac{\rho R^2_x}{E}[M]\{\ddot{d}\}+[K]\{d\}=\{P\} \tag{15}$$

where $[M]=[I]$, $[K]=[G_1]+[G_2][S]^{-1}[F]$. Solving the Eq. (2) under the boundary condition in Eq. (4), the stiffness matrix $[K]$ is a symmetric matrix. Set $\{d\}=\mathrm{Exp}(i\omega t)\{\phi\}$, we have the eigenvalue problem for natural frequency

$$\omega^2\frac{\rho R^2_x}{E}[M]\{\phi\}=[K]\{\phi\} \tag{16}$$

By using subroutines for eigenvalue problems in matrix forms, Eq. (16) may be solved with ease.

Since each components of matrices $[G_1]$, $[G_2]$, $[S]$ and $[F]$ are expressed in nondimensional parameters λ, μ, γ and Poisson's ratio ν, the matrix $[K]$ is also expressed in these quantities. Therefore, we find that natural frequency Ω for the flexural vibration of the shells are represented in the form

$$\Omega=\omega\sqrt{\frac{E}{\rho R^2_x}} \tag{17}$$

where the value of numerical factor ω is nondimentional frequency. These conclusions for the

shell also hold in natural frequencies for flexual vibrations of the shallow translational shells with any boundary conditions.

4. Numerical results

In order to examine linear behaviors of shallow translational shells with pinned support, we perform static analyses under uniform hydropressure load and the natural frequencies. The results show that the condition of inplane constraint has a great influence upon the behaviors of the shells, especially hyperbolic paraboloidal shells, and Poisson's ratio has considerable effects on the behaviors.

4.1 Static analyses

Setting $N=3,4,\ldots,11$ for the shell with $\gamma=1, \lambda=0, \mu=50, \nu=0$ under the uniform load, we examine the convergence of normal displacement and bending moment, and show the results in Fig. 2 where the displacement w_c and the moment M_x at the middle point are presented in the form

$$w(a/2, b/2)=w_c\times Pa^4/Eh^3, \quad M_x(a/2, b/2)=Mc\times Pa^2$$

In following static analyses, we adopt the number of serial numbers $N=10$. Then, setting $\nu=0$ and 0.3 for the shells with $\gamma=1, \mu=50$, we calculate w_c and the mean value factor $\overline{w}$ given by

$$\frac{1}{ab}\int_0^a\int_0^b w(x, y)dxdy=\overline{w}\times Pa^4/Eh^3 \tag{18}$$

and illustrate $\overline{w}-\lambda$ curves with solid lines and $w_c-\lambda$ curves with broken lines in Fig. 3.

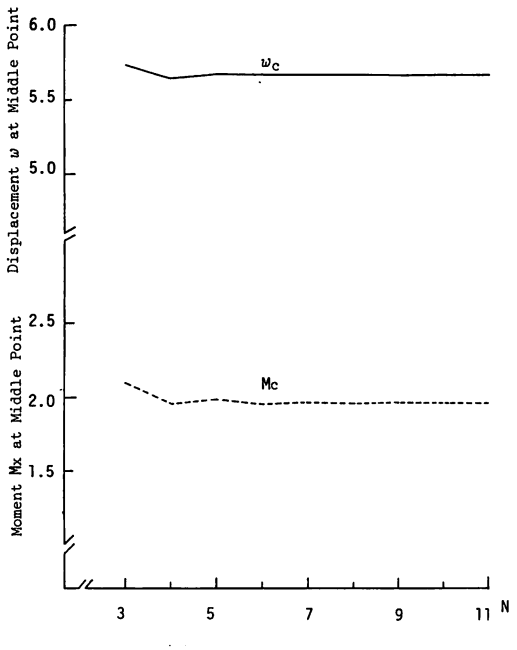

Fig. 2 Convergence of w_c and Mc

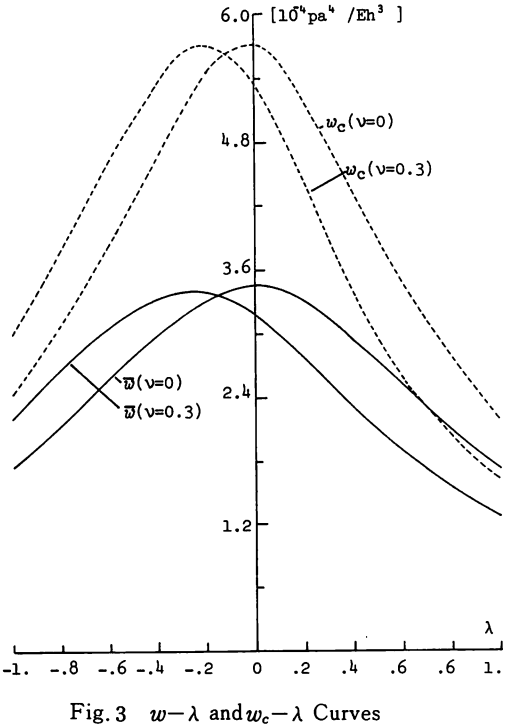

Fig. 3 $w-\lambda$ and $w_c-\lambda$ Curves

The displacement w and the bending moment M_x distributions along $y=b/2$ for three types of shells $\lambda=\pm1, 0$ with $\gamma=1, \mu=50$ and $\nu=0, 0.3$ are depicted in Figs. 4 and 5, respectively. When

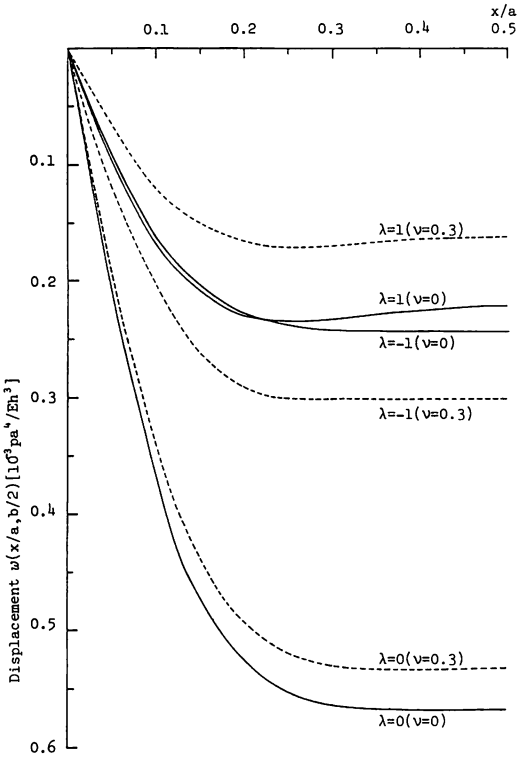

Fig. 4 Displacement Distributions

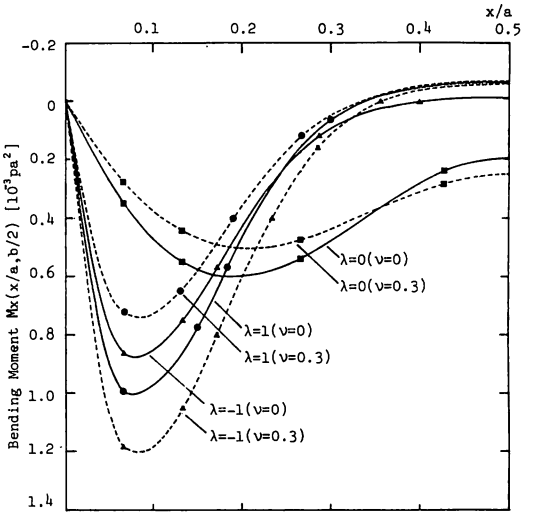

Fig. 5 Moment distributions

$\nu=0$, the displacement distributions for $\lambda=\pm1$ are analogous to each other, and the mean value of displacement $\overline{w}$ with λ in Fig. 3 is almost symmetric with respect to λ. In terms of w_c in Fig. 3 and M_x in Fig. 5, which are influenced by local deformations of shells, the behaviors of both shells with $\lambda=\pm1$ may be resemble. They permits us to get that when $\nu=0$, two shells with same absolute value λ show analogous behaviors. It is quite different from behaviors of shells with inplane inconstraint [3,11]. However, changing Poisson's ratio while all other parameters are unchanged, we notice the difference between the two shells. When Poisson's ratio is changed from 0 to 0.3, the whole curve of $\overline{w}-\lambda$ shifts almost parallel to the opposite direction of λ shown in Fig. 3, which indicates that $\overline{w}$ of the shells with $\lambda=1$ and -1 increases about -27 % and 26 %, respectively. The change of Poisson's ratio also makes the maximum bending moment M_x along $y=b/2$ for the shells with $\lambda=1$ and -1 increase -25 % and 35 %, respectively. Then, it is said that the increase of Poisson's ratio causes to decrease the whole displacement and the maximum bending moment for the shell $\lambda=1$, but to increase them for the shell with $\lambda=-1$.

4.2 Natural frequency analyses

Every eigenvalue ω^2 obtained from Eq. (16) is not only a square of natural frequency but also a eigenvalue of stiffness matrix with nondimensional parameters. Then, analyzing the natural frequencies make us assess effects of parameters γ, λ, μ and ν upon the matrix. Since Poisson's

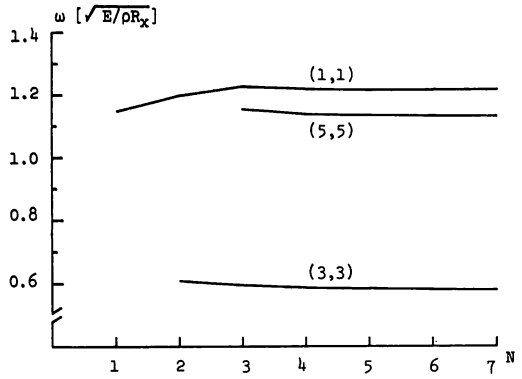

Fig. 6 Convergence of Frequencies

ratio has considerable influences on the behaviors of shells under uniform load with inplane constraint, we study effects of λ and ν on natural frequencies.

Setting $N=1,2,\ldots,7$ for the shell with $\gamma=1, \lambda=-1, \mu=160, \nu=0.3$, we examine the convergence of natural frequencies and show the results in Fig. 6. The notation (i, i) indicates that the natural frequency corresponds to the eigenvector in Eq. (16) where w_{ii} takes the maximum value. In following analyses, we adopt $N=7$.

Here, subscript i of the natural frequency ω_i is numbered in order to satisfy

$$\omega_1 < \omega_2 < \omega_3 < \cdots \tag{19}$$

and the eigenvector corresponding to ω_i is normalized with respect to the mass matrix in Eq. (16)

$$\{\phi_i\}^T[M]\{\phi_i\}=1 \tag{20}$$

For the shells with $\gamma=1, \mu=50, \nu=0$, the variations of ω_i with λ ($i=1,2,3,4$) are depicted in Fig. 7. The solid lines correspond to the eigenvectors where w_{11} takes the maximum, which exists

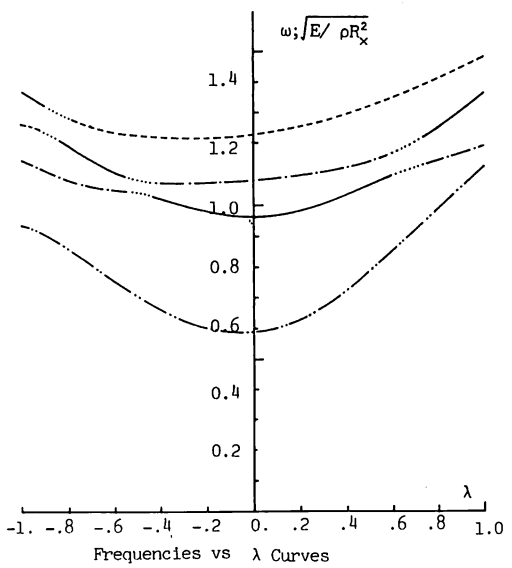

Fig. 7 Frequency ω_i with λ Curves

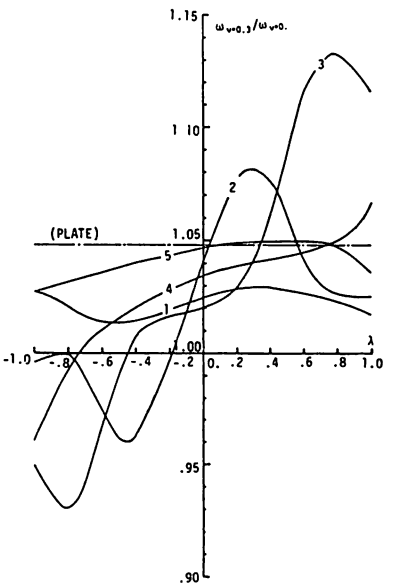

Fig. 8 Frequency ratio with λ Curves

on the curve for ω_2 when $\lambda=0$. However, the solid line is found on the curve for ω_3 in the neighborhood $|\lambda|=0.8$. Then, there are transitions of modal configuration presented by eigenvectors between the natural frequencies ω_2 and ω_3 in the neighborhood regions $|\lambda|=-0.6$. The transition of modal configuration is also found between ω_3 and ω_4 in the region $\lambda=-0.8$. The phenomenon suggests that natural frequencies of shells are not traced by modal configurations.

In order to examine effects of Poisson's ratio on natural frequencies, we analyze the shell with $\nu=0.3, \gamma=1, \mu=50$ and the shell with $\nu=0, \gamma=1, \mu=50$, and present each ratio of former natural frequency $\omega_i|_{\nu=0.3}$ and latter one $\omega_i|_{\nu=0}$ with λ, denoted as $\omega_{0.3}/\omega_0-\lambda$ curves, in Fig. 8 where the numbers written on each curve indicate i defined in Eq. (19). For every natural frequency of plates, the ratio becomes $(1-\nu^2)^{-1/2}|_{\nu=0.3}=1.0483$. From Figs. 7 and 8, it is found that each natural frequency on which changing Poisson's ratio has a considerable influence may corresponds to the eigenvector where w_{11} takes the maximum. The eigenvector has the modal configuration having the maximum volume change in eigenvectors. Therefore, we may say that the increase of Poisson's ratio lets increase the natural frequency corresponding to the eigenfunction with the maximum volume change for the shells in the region $\lambda>0$, especially for the shell in the neighborhood region $\lambda=1$, and lets decrease the natural frequency for the shells in the region $\lambda<0$, especially for the shell in the neighborhood $\lambda=-1$.

The eigenvector with the maximum volume change may have the maximum membrane energy in eigenvectors of the shells. So for the shells with $\gamma=1, \mu=50, \nu=0$, we seek the membrane energy for each eigenvector, and show its factor V defined bv

$$\frac{1}{2}\int_0^a\int_0^b \frac{1}{Eh}\{N^2_x+N^2_y-2\nu N_xN_y+2(1+\nu)N^2_{xy}\}\,dxdy=V\times Eh^3/a^2$$

in Fig. 9, where the number written on each curve indicate i in Eq. (19).

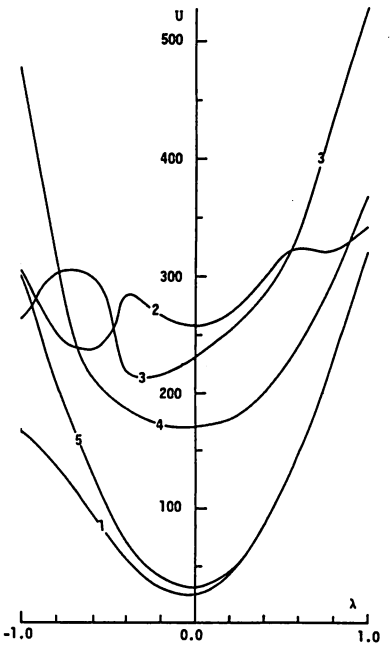

Fig. 9 Membrane Energy with λ Curves

Judging from Figs. 8 and 9, it may be said that the effects of changing Poisson's ratio on the shell natural frequency corresponding to the eigenvector with the more membrane energy differ from the effects on plate natural frequencies.

Conclusion

Linear behaviors of shallow translational shell with pinned support along edges are studied. The results of static analyses under uniform load are summarized as follows

1. When Poisson's ratio is zero, the whole displacement of the spherical shell ($\lambda=1$) and the hyperbolic paraboloidal shell ($\lambda=-1$) are resemble.
2. The increase of Poisson's ratio makes degrease the displacement and the maximum bending moment for the shell with $\lambda=1$, but makes increase them for the shell with $\lambda=-1$.

The results of natural frequency analyses are summarized as follows

3. The effects of changing Poisson's ratio on the shell natural frequency corresponding to the eigenvector with the more membrane energy differ from the effects on the plate natural frequency.
4. The increase of Poisson's ratio makes increase the natural frequency corresponding to the eigenfunction with maximum volume change for the shell with $\lambda=1$, but makes decrease the natural frequency correponding to it for the shell with $\lambda=-1$.

References

1) 坪井, 高橋 "周辺固定支持されたH. P. シェルのフーリェ解析" 日本建築学会論文報告集第104号 昭和39年
2) 中田, 坪井 "偏平HP およびEPシェルのフーリエ弾性解析" 日本建築学会論文報告集第318号 昭和57年
3) 清水, 真瀬, 伊藤, 和泉 "偏平推動殻の応力分布へ及ぼす曲率の影響" 建築学会東北支部 昭和52年
4) 横尾, 国枝 "偏平シェルの振動(Ⅰ)" 及び(Ⅱ) 日本建築学会論文報告集第114号 昭和40年
5) H. Kunieda "Solutions of Free Vibrations of Spherical Shells" 日本建築学会論文報告集第325号 昭和58年
6) E. Reissner "On Transverse Vibrations of Thin, Shallow Elastic Shell" Q. Appl. Math. 13, 1955
7) K. Apeland "Stress Analysis of Translational Shells" A. S. C. E. EM 1 p. 2743, 1961
8) A. W. Leissa and A. S. Kadi "Curvature Effects on Shallow Shell Vibrations" J. Sound Vib. 16, p. 173, 1971
9) K. Kanazawa and Y. Hangai "Nonlinear Flexural Vibration of Thin Shallow Shells" Proc. 25th Japan National Congress for Applied Mechanics, 1975
10) 皆川 "Vlasov 型基礎式に基づく面内変位を抑えた偏平シェルの解析" 建築学会大会 昭和57年
11) 坪井善勝 "連続体力学序説" 産業図書